

Vehicle-to-Grid Coupled Photovoltaic Optimization for Singapore at a District Resolution

Dominic Caviezel^{a,*}, Christoph Waibel^{a,*}, Markus Schläpfer^b and Arno Schlueter^a

^a *Architecture and Building Systems (A/S), ETH Zurich, Switzerland, waibel@arch.ethz.ch*

^b *Civil Engineering and Engineering Mechanics, Columbia University, New York, United States*

Abstract:

This paper investigates the potential of building attached / integrated Photovoltaic (PV) and vehicle-to-grid (V2G) coupling for the city of Singapore. Using the city's 55 planning areas as spatial units, a linear programming (LP) optimization model is developed to determine economically optimal PV scaling and charge/discharge strategies within and across planning areas. Mobility flows between planning areas are assessed using a large set of GPS mobile phone records, from which electric vehicle (EV) schedules are derived. Local electricity demand and solar potentials are modelled using a bottom-up approach based on building geometries and land use information, and loads are calibrated to match measured aggregate city loads. Parametrized assumptions in our model are systematically tested through scenario analysis, including varying carbon taxes, PV system cost, EV penetration, wholesale electricity prices, and local building self-consumption levels. Our study finds significant economic and environmental potential for PV systems, while economic benefits of V2G are strongly scenario dependent but generally limited. This may be explained by the high on-site PV electricity self-consumption potential due to the electricity loads generally exceeding PV generation. However, through the aggregation to the planning area level in our model, local building-resolved mismatches in production and demand were partially flattened, and thus the potential for V2G to act as intermediate storage can be expected to be higher when modelled at a finer spatial resolution. In order to gain further insight, future research could focus on combining large-scale city dynamics with more fine-grained local analysis, e.g., by limiting the analysis to one district only, as well as incorporate explicit grid balancing constraints in the model.

Keywords:

Vehicle-to-grid, Photovoltaic, Linear Programming, District Energy, Optimization.

1. Introduction

Substituting fossil fuel-based energy generation with renewable sources, such as Photovoltaics (PV), and the promotion of electric vehicles (EV), are two of the key measures to decarbonisation [13]. The aim of this paper is therefore to investigate possible synergies between the two technologies, PV and EV, and study the impact on energy-related cost and emissions if vehicle to grid (V2G) technologies were widely adapted at a city scale. V2G relies on bidirectional chargers allowing EVs not only to charge their batteries but also discharge stored electricity back into the grid. In this capacity they can be used as temporary storage devices for excess electricity from renewable sources, participate in electricity arbitrage or even increase grid stability by providing ancillary services.

1.1. V2G at a city scale

With the development of EVs as a potentially low carbon alternative to vehicles with internal combustion engines (ICE), research has investigated their integration into the existing infrastructure. One area of concern is the impact of large-scale EV adoption on grid stability, with studies highlighting the importance of charging speed [25] and grid-related benefits of nighttime off-peak charging [18]. Control schemes can be specifically designed to avoid grid overloads [7], or to optimize for either user preferences or grid cost [23]: When optimizing for user preference (i.e., optimal state-of-charge, SOC, for mobility demand), electricity may be drawn from the grid during peak demand, leading to potential shortage concerns, whereas a grid-cost minimization can relax the load on the power system. Smart charging strategies are therefore central to successfully combine EVs with the intermittent production of renewable energies such as PV. The objective of coordination is often to increase the self-consumption of locally produced PV-electricity by storing excess production in EV-batteries [10].

Further increasing synergies between local production and EVs is attempted through bidirectional charging. Energy stored in the EV battery can be discharged and consumed on site or fed back into the electricity grid

*These authors share first authorship.

(V2G). In this capacity vehicles can deliver stored PV energy at times of high demand or high electricity prices or even provide ancillary grid services. Such concepts have been explored at the level of individual homes [8] or in more aggregated forms such as parking lots [21]. At larger scale and with a focus on generating realistic EV mobility patterns, Lin et al. (2018) [16] developed a multi-agent system to test the impact of different charging schemes on a generated energy hub. By defining the behavior patterns of different agents (EVs, coordinators etc.), an attempt was made to model realistic behavior patterns including parking duration and charge probability. The study found that peak demand increased under uncontrolled charging scenarios, but through coordinating behaviors the demand could be pushed into the valley period. When V2G was employed the overall electricity demand increased significantly, but the operation of a supplementary gas turbine could be reduced and heating and cooling costs fell significantly suggesting synergies between technologies.

V2G analyses at the city scale are scarce in the existing literature. One example is Kobashi et al. (2020) [15], where the authors looked at PV and V2G interactions for the entire city of Kyoto with real world data. A techno-economic analysis was conducted using hourly electricity demand and PV production at a city aggregate resolution. Significant environmental and economic benefits were found when both technologies, PV and V2G, were deployed in conjunction with each other. The study estimates average mobility patterns from survey information and derives gasoline use and park times. However, due to the aggregation to the city level, local mobility patterns or energy demands are not differentiated in the analysis.

1.2. Mobility flows from mobile phone data

Several studies employ mobile phone data to generate mobility patterns. This data can be obtained for a large fraction of the population and is available in locations where other forms of statistics may be limited. Iqbal et al. (2014) [14] demonstrate that mobility flows can be captured in the form of origin-destination matrices using mobile phone Call Detail Records (CDR) and minimal traffic information without the need for detailed demographic and mobility statistics. As such CDR data can also be used for traffic or infrastructure planning in developing countries where data availability is low [9].

Mobile phone data has also been employed in relation to EV technology. Vazifeh et al. (2019) [26] used CDR data of one million users to determine the optimal positioning of charging stations in Boston. To the authors' knowledge Schläpfer et al. (2021) [24] have been the only ones to use mobile phone data to assess local V2G charging and discharging patterns and relate it to V2G infrastructure planning. The data used is not CDR data but collected from a variety of apps. This allows for the implementation of different tracking modes and offers the potential for more complete movement patterns. Using Singapore as case study, the city-state was separated into a grid of 250m-by-250m cells and a trajectory for each user was derived as their recorded locations moved to different cells. From these trajectories aggregate movement patterns were determined which were then translated to EV vehicle movements. Simple, uncoordinated charging schemes were deployed, where users preferably charged their vehicles during the sunny hours and discharge at night, maximizing PV consumption. It was assumed that charging and discharging was possible in any location where a user stayed for more than one hour.

The study found that a large part of the electricity was discharged outside of residential neighborhoods in primarily commercial zones such as the Singapore Downtown Core. This contradicts the assumption that V2G can mainly provide electricity to residential areas and encourages the inclusion of complex mobility patterns in research. Household electricity was estimated and compared to V2G output assuming that 3% of the mobility flows were covered by EVs. It was found that districts could cover up to 40% of the nighttime household demand using V2G, although most districts fell between 10% and 20%. Comparing charging demands to a simple estimate of PV potential found that local PV alone could likely not cover peak charging demands, requiring other solutions such as smart charging or grid imports.

1.3. Contributions

PV and V2G are both essential elements of the Singapore Green Plan 2030 published by five government Ministries as an outline towards the ecological transformation of the city-state [20]. The plan sets several concrete targets to be reached by 2030. Included is the target to increase electric mobility by providing 60'000 EV charging stations throughout the island and the target to install 2 GWp of PV capacity (system peak demand in Singapore by 2030 is projected to be 9 GW [1]). In this context, Singapore provides a good case for studying the integration of PV and V2G. Therefore, the following research questions are investigated in this paper:

- How does the penetration of EVs and V2G technologies affect optimal scaling of building attached / integrated PV systems, as well as cost and emissions of electricity?
- What levels of self-consumption and self-sufficiency can be achieved at a district scale?
- What is the impact of different boundary conditions, including local (i.e. building) self-consumption rates, carbon taxes, PV system cost, EV penetration, and wholesale electricity prices on cost, emissions and PV capacities?

The specific contributions are:

- As compared to Kobashi et al. (2020) [15], we increase the spatial resolution to the district scale in order to capture local effects of a heterogeneous system.
- Building on Schläpfer et al. (2021) [24] as a first assessment of PV and V2G potential, we now investigate economic feasibility in our study.
- Using a similar method for V2G mobility flow assessment, our study includes economic factors to assess feasible PV scaling and optimal charge/discharge patterns in various scenarios.
- We also estimate and implement the full electricity load of Singapore at planning area scale and not just total household demand.
- Finally, building energy demand and PV potentials for rooftops and facades are estimated using bottom up simulations at a high 3D spatio-temporal resolution.

2. Methods

We develop a linear programming (LP) optimization model for the techno-economic investigation of optimal PV scaling and EV charge / discharge schedules at the level of the 55 planning areas of Singapore. The LP is described in section 2.1. and illustrated in Fig. 1. Other methods employed center around the LP to generate following relevant spatio-temporal input data: electricity demand (section 2.2.), solar potentials (section 2.3.), and mobility patterns (section 2.4.).

2.1. Optimization model

The LP model captures electricity, cost, and emission flows for each of the 55 planning areas in Singapore. The temporal resolution is one hour. Calculations are made for one year. However, due to computational constraints only four representative weeks were modeled. These were derived by clustering similar weeks together. Results for each modeled week were then multiplied by the number of weeks in that cluster in order to scale up to a full year. For each district a set of electricity consumers and producers with associated electricity flows was defined. Three main components are included: Buildings, PV Systems, and EVs. Fig. 1 shows the basic structure of the model.

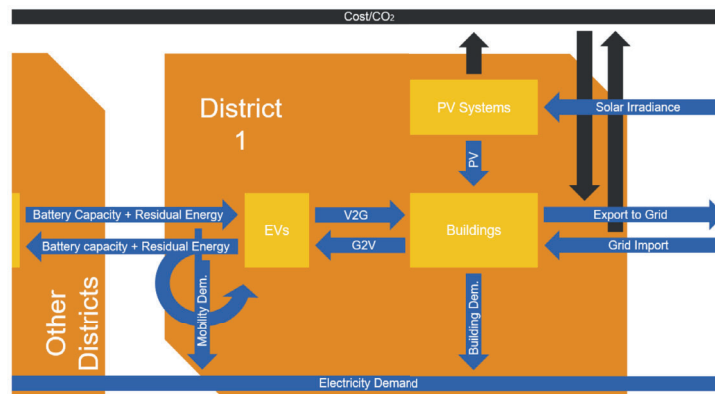


Figure 1: Overview of the LP optimization model. Blue arrows represent electricity flows, black arrows monetary flows and emissions. Yellow boxes represent the main actors contained in the model, orange defines planning area borders.

The majority of consumption in each planning area can be associated to buildings, with modeled demand described in section 2.2.. The main way of meeting the building demand is through grid imports with associated costs and emissions. Alternatively, demand can be met through installed PV systems. Unlike grid imports, PV systems do not incur costs per kWh but rather one time installation and yearly operational costs irrespective of electricity produced. The LP model can optimally scale PV over potential areas, deciding where it is financially viable to install systems. Produced power that exceeds the local demand of a planning area can be exported through the national grid. Exported PV generates revenue. Singapore offers contestable consumers the option to buy and sell electricity at the wholesale electricity price (WEP). For modeling, this WEP was taken as the basis for trading.

The final component represents EVs. When stationary, they can be charged or discharged using V2G. Discharged electricity is fed back into the local energy balance and can be consumed within the planning area

or be exported through the national grid. When EVs drive from one district to another they carry their battery capacity as well as the electricity stored in their battery with them. Since the spatial resolution is the planning area, all EVs in a location at a given time are represented by a single battery and are assumed to have the same state-of-charge (SOC). If an EV enters a district with lower charge, the energy difference is subtracted from the representative battery, and EVs with higher charge add their excess energy to the local battery. Electricity consumed by driving is subtracted from the EVs battery.

The objective function of the LP represents total costs associated with Singapore's electricity flows to meet the total electricity demand and aims to maximize revenue:

$$\max_{x \in \mathbb{R}} (f_{\text{Export}} - f_{\text{Import}} - f_{\text{GridFee}} - f_{\text{PV}}), \quad \text{s.t. } x \in \Omega, \quad (1)$$

where x include operational variables for power flow within and between planning areas and design variables for installed PV per planning area and different orientations (North, East, South, West, roof), and Ω are the system constraints describing the energy balance and technology behavior. f are linear expressions describing revenue generated from generated PV electricity or discharged electricity exported to the grid, as well as cost occurring from imported grid electricity, market support charges on grid transmissions applied to imports and to a fraction of local production to account for local transmission within planning areas, and annualized PV installation cost. Grid carbon emissions are additionally priced with a carbon tax. Prices are obtained from EMC (2022) [6]. A complete formulation and list of parameters and model constraints can be found in Caviezel (2022) [4]. The model was generated using the Python package Pyomo and solved using Gurobi.

2.2. Building energy demand modeling

The electricity demand for each planning area was modeled with a bottom-up approach using the energy modeling software City Energy Analyst (CEA) [11]. The open-source tool can determine different energy related time series for individual buildings based on building attributes, weather input, and site surroundings. A pre-populated database with building archetypes and demand schedules exists for Singapore. For accurate modeling, several attributes were derived for each building in Singapore. For the rest of the variables, CEA-defaults were used.

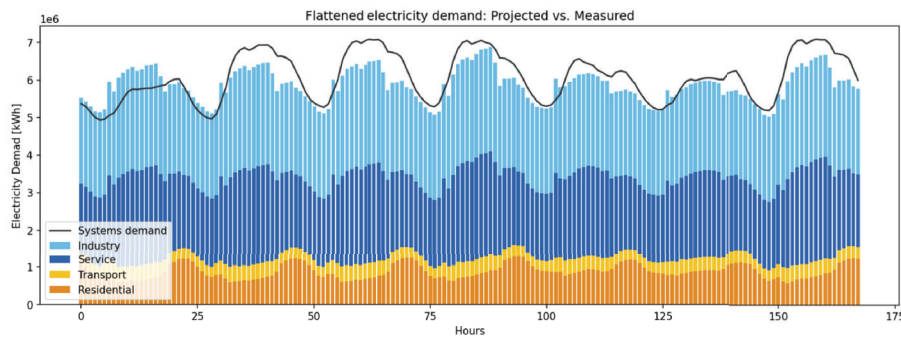


Figure 2: Modeled electricity demand by sector after scaling and amplitude adjustment vs the total systems demand. Period shown is January 1st to January 7th 2019.

2.2.1. Missing building heights

Individual building polygons with height and use type information were obtained from Open Street Maps and data from the Urban Redevelopment Authority (URA), resulting in a total of 111'485 buildings. Only 21'755 of the buildings had associated height information. We estimated the height of the remaining buildings using a feed-forward artificial neural network (ANN), using the Keras library. After testing different ANN architectures and manually tuning hyper-parameters, the final model resulted in a mean absolute error of 4.64 m and an R-squared value of 0.75, indicating significant correlation. Considering Singapore's large share of high-rise buildings, we consider the error to be acceptable.

2.2.2. Clustering

Due to computational constraints, instead of simulating the 111'485 buildings of Singapore explicitly, we clustered them into groups, similar to the approach taken by Murray et al. (2020) [19]. We used the following 5 attributes for clustering: (i) building use type, (ii) number of attached neighbouring buildings (0, 1, 2 and more), (iii) total floor area, (iv) envelope to volume ratio, and (v) height/distance ratio to neighbouring buildings (sum of the height of each neighbor divided by the distance to that neighbor). The clustering resulted in a total of 445

differentiated groups, representing combinations of the categorical attributes (i) and (ii). For each cluster, the energy demand of the central sample was modeled in CEA and using a typical meteorological year weather file for 2020 as generated from `MetEonorm`. To represent shading effects, for each modeled building (i.e., cluster centroid), neighboring structures within a 50m radius were included as surroundings.

2.2.3. Calibration

To correct for the mismatch between simulated and actual electricity loads, the load curves were calibrated to measured load curves. We could only find specific hourly loads for the residential sector in Raman & Peng (2021) [22], representing aggregated loads of over 10'000 residential buildings. The demand curves of these measured and aggregated profiles were found to have a smaller amplitude and the evening peak occurred later than in the CEA profiles. Additionally, some days had a morning peak, others did not. The latter were assumed to be weekends when inhabitants did not need to go to work. By adjusting the appliance, lighting and hot water loads in CEA, a custom demand profile was generated which better matches these measured profiles.

The Energy Market Authority (EMA) publishes the annual electricity consumption by sector [3]. The previously generated building demands were summed by sector and compared to these published values. The energy use intensities (EUIs) of service, residential, and industry sectors were scaled to match annual values for 2019, which was chosen as the year before the COVID-19 pandemic, where demand was not yet skewed.

High resolution demand information summed over the entire island is published by EMA in form of half hourly systems demand. After scaling the modeled profiles to match the yearly demand, the systems demand was used to assess hourly load distribution. It was found that the timing of minimum and maximum loads matched well, however the amplitude of the modeled demand curve was much higher than that of the measured systems demand. These differences were corrected by scaling the energy demands around their individual means. Fig. 2 shows the final, adjusted demand for the same period in January 2019. To get local hourly demand curves, the adjusted demands for all buildings in a planning area were summed.

2.3. Solar modeling

Hourly solar irradiation for all building surfaces (roof and façade) was simulated on a 0.7m × 0.7m grid, resulting in several million hourly solar profiles for the whole city of Singapore. The same weather file as for the building demand simulation is used. Building geometry information was taken from `Open Street Maps`, and data was kindly provided by researchers from Singapore [2]. The sum of geometrically available surface area per category and planning area was adjusted according to scaling factors found in the `SERIS PV Roadmap (2020)` [1] in order to get area suited for PV installations. Scaling factors are dependent on building and surface type and were correlated to the sectors assigned in section 2.2.. Since using several million solar profiles would lead to excessive computing cost in the optimization model, solar profiles were clustered into 5 categories (North, South, East, West, roof) for each of the 55 planning areas respectively using k-Medoids. Thus, per district, 5 annual hourly solar profiles were utilized in the PV sizing optimization to represent the bulk aggregate surface areas for each orientation. The software `ClimateStudio`, which is a plug-in for the CAD program `Rhinoceros 3D`, was used for simulating solar irradiation. An excerpt of the simulation results is shown in Fig. 5a.

2.4. Mobility patterns generation

To estimate local battery capacity, mobility demand, and the movement of residual energy in EV batteries, mobility patterns were derived. Continuous patterns for one week were generated from a dataset of individual mobile phone logs.

2.4.1. Dataset

A dataset containing mobile phone records collected from September 1st to September 30th, 2020 was obtained from `Citydata` [5]. During the 30-day period a total of 108'971'459 logs were captured. Each log contains a user ID, GPS coordinates and a timestamp. A total of 1'291'343 unique users are registered. The set covers the whole island of Singapore. The number of logs captured varies throughout the month and throughout each day (Fig. 3 (A)). 4:00 to 5:00 is the hour with least activity. This hour was therefore chosen as starting and ending time for all modeling periods in order to minimize period overlapping activity. The data was collected from users of a wide variety of mobile applications with a geospatial component. `Citydata` provides application developers with an add-on software component which records anonymized location data. Different tracking modes and log frequencies can be set by developers ranging from "manual" where records must be manually triggered to "HawkEye" with continuous tracking. According to `Citydata`, around 80% of developers chose "stay detection" which is triggered by the crossing of geofences and thus mainly captures movement (Yeow Leong Lee, personal communication 22.6.2022). The frequency of registrations for individual users varies strongly. Often, bursts of logs are followed by long periods without records. Other users are captured once and then disappear from the dataset (Fig. 3 (B)). Due to the prevalence of "stay detection" tracking, an assumption can be made that in many cases movements are recorded and periods without logs indicate that users remain stationary. The recording mode of individual logs is not indicated in the dataset.

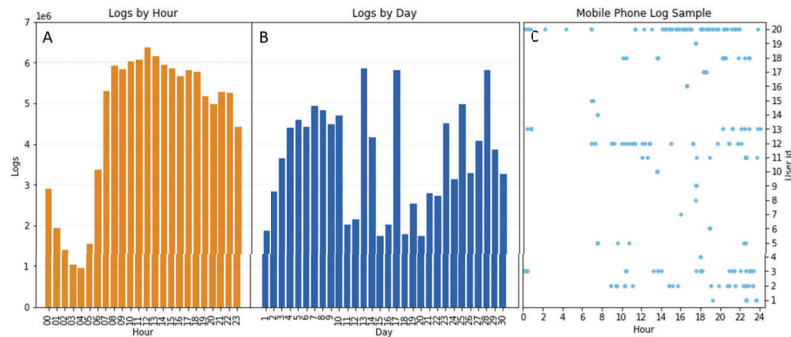


Figure 3: Mobility dataset overview. (A) Cumulative logs contained in the dataset by hour of the day. (B) Cumulative logs by day of the month. (C) Registration times for a random set of users.



Figure 4: (A) Schematic of the routing algorithm. Movement takes place from left to right. Points are classified into route points (orange) or intermediate points (black). (B) An example route generated using OSRM starting at the location of the green waypoint and ending at red. Blue waypoints are routing points, grey ones are intermediate points.

2.4.2. Generating trajectories

In order to generate mobility patterns for a full week, the data was separated into four one-week periods starting on September 2nd, 9th, 16th, and 23rd. Weeks were analyzed separately and later merged. One day before and one after each period were considered for establishing the start and end location of the users. For each time period, only users who had at least one log per day were considered to be reliably tracked and processed further. A total of 56'794 unique IDs remained.

For each user an hourly trajectory was generated. Individual user logs were categorized into route points and intermediate points. The route points were used to determine user trajectories while intermediate points were dropped from further analysis. The first registration of a user in a period was taken as the first route point. Subsequent points were classified as route points if the direct distance to the last route point exceeded 500m or planning area boundaries were crossed. Fig. 4 (A) shows this in a schematic form. Starting with the first orange route point on the left and moving right, points are classified into route points (orange) or intermediate points (black).

Real world driving paths between route points were generated using the open-source routing machine OSRM [12]. OSRM also provides an estimated driving duration. The registration time of a route point was taken as the arrival time at its location. From this the estimated driving duration was subtracted to get the departure time from the location of the last route point. To match with the time resolution of the LP, users were classified as moving during hourly time steps where they either departed, continued a trip, or arrived at a new destination. During full hours with no movement, users were considered to be stationary and associated with EVs available for charging or discharging. Finally, the routes from all four weeks were combined into one aggregated week. As it is assumed that users follow similar mobility patterns throughout the different weeks, users tracked in multiple weeks were weighted accordingly. Movements by a user included in three of the four weeks were therefore only counted as one third in each of these three weeks.

2.4.3. Anomalies

In occasional cases, logs from individual IDs were observed to jump between far apart locations in very short intervals. In Singapore, car traffic is limited to 90 km/h and the public transport lines do not exceed 100 km/h. A maximum speed of 120 km/h with respect to the direct distance of two log points is therefore set as an upper limit. Logs implying speeds above this threshold are assumed to be GPS anomalies and are not counted as route points. A second anomaly was detected in relation to routing. Occasionally, routes generated by OSRM follow long and unintuitive paths between two route points. This is generally the case when points do not follow

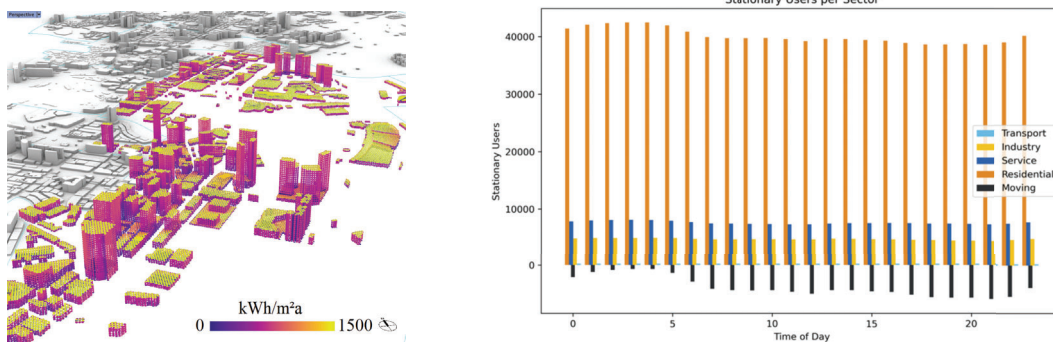
the road layout either because the user is taking another mode of transport (e.g. walking or train) or due to GPS inaccuracies. To reduce exaggerated distances and travel times, routes with route distance of more than 2.5 times the direct distance were corrected to have the average ratio between direct distance and route distance. Travel times were adjusted accordingly.

3. Results

3.1. Inputs to Optimization

Fig. 5 and Fig. 6 shows some of the inputs used throughout the studied optimization scenarios. In Fig. 5a, an excerpt of the 3D solar simulation is shown. According to our simulations, PV on buildings can generate up to 15.2 TWh of electricity with 14.2 GWp capacity installed, assuming a conversion efficiency of 20% and an installation threshold of 500 kWh/m²a solar irradiation on surfaces (see Fig. 3 in Waibel et al. 2021 [27] for feasible thresholds in Singapore based on optimization). Alternatively, with a threshold of 750 kWh/m²a, we can achieve a generation potential of 11 TWh and a capacity of 7.5 GWp. This compares well to the SERIS PV roadmap [1], which reports a capacity of 8.6 GWp at 750kWh/m²a threshold, but also including PV on infrastructure and floating PV. The total electricity demand of Singapore for 2019 was reported to be 51.7 TWh, where the industry sectors accounts for 21.5 TWh (41.5%), the commercial and service sectors for 19.3 TWh (37.3%), households for 7.7 TWh (14.8%), and the transport sector for 3.0 TWh (5.8%) [3] (Fig. 6a). Therefore, PV on buildings could potentially cover 21% (750 kWh/m²a threshold) or 29% (500 kWh/m²a threshold) of total annual electricity demand. In this paper, however, the optimization model will decide on the actual PV capacities installed per district.

The annual electricity demand per floor area and planning area is shown in Fig. 6c; the annual solar irradiation is shown in Fig. 6b. Districts dominated by transport have the highest average irradiation of 808 kWh/m²a, followed by Industry with 796 kWh/m²a and Service with 756 kWh/m²a. Planning areas with mainly residential buildings have the lowest average solar irradiation per area with 663 kWh/m²a. As for electricity demand, values vary significantly across planning areas, with residential electricity demand intensity being the lowest and industrial the highest.



(a) Annual solar irradiation on roof and facades around Downtown Singapore.

(b) Non-stationary users on the negative axis, and stationary users by predominant sector of the planning area they are located in.

Figure 5: Inputs to the optimization: solar potentials and mobility patterns.

Fig. 5b portrays users tracked in the mobility dataset classified as stationary or parked. Planning areas are grouped by predominant sector. Users in motion are plotted on the negative axis. A distinct driving pattern can be observed with lowest activity during the night hours and peaks in the morning and evening. However, shifts of occupancy between sector types throughout the day are minimal. Planning areas of all sector types have their highest occupancy levels at night. These drop during the day. The sum of users is constant, drops in overall stationary users represent users on the move.

3.2. Scenario Analysis

Multiple scenarios were generated by deviating individual parameters from a base scenario. The base scenario reflects targets of the Singapore Green Plan 2030 [20]. Where possible, parameters were modified to represent either current values (low environmental considerations) or targets and predictions for 2040 (high environmental considerations). Amongst others, local self-consumption (LSC) [17] is used as a parameter in our study. It is defined as PV electricity consumed directly by an individual building. Excess electricity needs

to be sent through the local grid, even if it is reconsumed within the same planning area in which case grid charges apply. The LSC factor attempts to correct for this effect by applying scaled grid transmission charges to electricity transferred within a planning area. The charge is applied to all local production (PV and V2G) but is reimbursed when electricity is exported outside of the district, as in this case the full transmission fees are paid in the planning area where the electricity is imported to. In contrast, *district level* self-consumption (SC) is a dependant variable in our study and calculated with $d_{w,t,l}^{total} = d_{w,t,l}^{building} + x_{w,t,l}^{charge} - x_{w,t,l}^{discharge}$, where x are operational decision variables for charging and discharging batteries (including EVs), d is demand, and w, t, l are indices for week, timestep (hours), and location (district). Detailed and complete parameter values are reported in [4]. Fig. 6d to 6i show the fraction of PV production exceeding local demand at a time of production, district

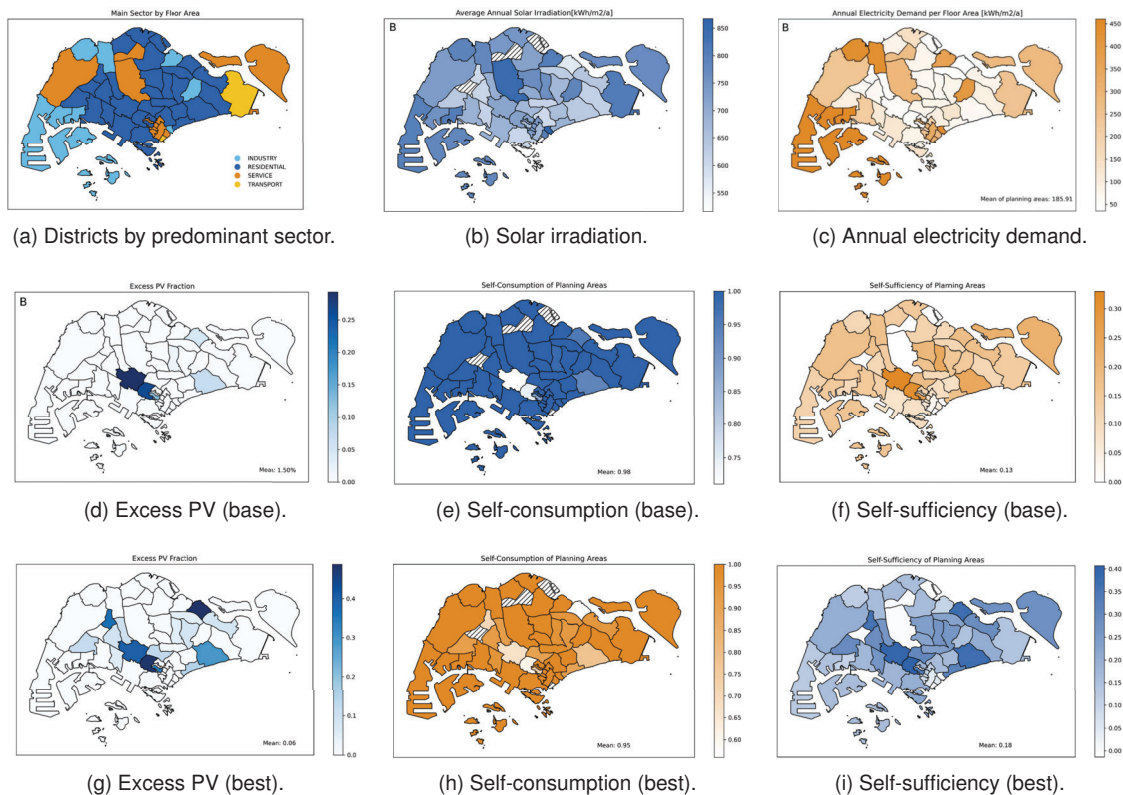


Figure 6: Singapore with results shown by planning area. Diagonal lines mark districts where no data was registered.

level self-consumption, SC, and district level self-sufficiency* for the base scenario and an (environmentally) *best case* scenario. In the base scenario a LSC value of 40% is chosen (between typical self-consumption values without storage and values with dedicated storage found in [17]) and in the best case scenario 80% an optimistic value still found in the literature, since Singapore has high demand compared to its PV production capacity. In the base scenario, the pre-pandemic WEP from 2019 was chosen as a stable baseline. By 2022 the WEP had risen by a factor of 2.8. This was used as a multiplication factor to generate the best case WEP from that in the base scenario. Additionally, full EV-penetration (600'000 EVs) was implemented compared to 10% penetration in the base scenario. In the best case scenario the fraction of excess PV increases to an average of 6% under the best-case scenario with complete utilization of surface potential. All of this is found in predominantly residential planning areas where the average is 10% with values reaching up to 49%. Excess in other sectors is negligible. Self-consumption remains high with 95% and a range from 100% to 56%. Self-sufficiency averages at 18% but can reach levels of 40% in districts where PV production is high compared to local demand. It should be noted that, when running a scenario without V2G, the effect on average planning area self-consumption and self-sufficiency was minimal with V2G increasing self-consumption by about 0.5% and self-sufficiency by 0.03%. This can be explained by the generally already high levels of SC where EV

*Self-consumption represents the fraction of PV consumed locally while self-sufficiency describes the fraction of local demand covered by PV.

electricity demand is negligible in comparison to total electricity demand.

3.2.1. Scenario Comparison

Fig. 7 shows a comparison of all studied scenarios and the difference in system cost, optimal PV capacities, and CO₂ emissions. Following parameters are used in the various scenarios: CO₂ tax in S\$/tCO₂eq. = 0 (low), 60 (base), 95 (high); EV penetration in number of EVs = 3000 (low), 60'000 (base), 600'000 (high); PV CAPEX = estimates from 2022 (low), 2026 (base), 2031 (high) as from [1]; wholesale electricity price (WEP) = prices from 2019 (base), base × 2.76 (high), base × 0.5 (low); LSC in % = 20 (low), 40 (base), 80 (high). Furthermore, some scenarios are calculated with or without PV, and with or without V2G. The colorbar range is set to -30 to +30 %, but numeric values are indicated in the cells.

Results show that increasing LSC made PV systems significantly more viable with investment increasing by 257 Mio S\$ or 59%, decreasing self-consumption reduced investment by 42 Mio S\$ or 10%. Installed PV capacity reached 8.6 GWp (57% higher than in the base scenario), import related costs decreased significantly and export revenue increased with higher levels of self-consumption. Electricity related CO₂ emissions are reduced by 0.6 Mt/a in a high LSC scenario, while they marginally increase by 0.1 Mt/a in a low LSC scenario. In summary, achieving high degrees of high LSC shows both significant economic and environmental benefits.

In all scenarios PV installations are able to significantly reduce costs and emissions of the Singapore electricity market. The optimal installed capacity determined by the model ranges from 4 to 14 GWp depending on the scenario. Under the base assumptions for 2030, the optimally installed capacity is 5.5 GWp. As such, economically viable PV potential is significantly larger than the 2 GWp capacity targeted set in the Singapore Green Plan 2030 [20]. Under base scenario assumptions PV systems can reduce carbon emissions from electricity generation by around 3 Mt or 15% compared to the same scenario without PV.

The impacts of V2G are strongly scenario dependent. In the base scenario cost reductions due to V2G technology come to only 7 S\$ per EV and year. Savings can be increased up to 127.65 S\$/EV/a under the best-case scenario. The economic potential of V2G for self-consumption increase and electricity arbitrage is therefore severely limited in all scenarios. Additionally, V2G increases CO₂ Emissions in the base and best-case scenario by increasing the overall electricity imported. Synergies between PV and V2G are minimal although V2G does increase the economically viable PV area in one scenario (High LSC w/o V2G to High LSC scenario).

3.2.2. Demand vs PV production

Fig. 8 shows average hourly building energy demand and PV production with optimal capacities from the base scenario for a predominantly residential, industrial, and service dominated planning area, respectively. It is striking that only in the first district, PV production exceeds demand, while in most other districts PV electricity can only provide a fraction of total demand. Considering that the majority of total electricity demand stems from industry and service/commercial use, most districts will not be able to export PV (also see Fig. 6d and 6g). For the commercial- and service sector, this is due to the constantly high cooling loads throughout the year.

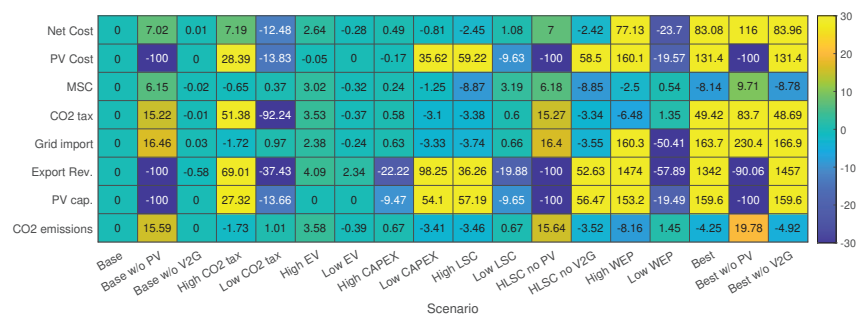


Figure 7: Comparison of all studied scenarios with values shown as % deviation from the base scenario. Net cost = PV Cost + MSC + CO₂ tax + Grid import - Export revenue; MSC = market support charge; HLSC = High LSC; WEP = wholesale electricity price.

3.2.3. Charging Schedules

Two modes of EV charging can be differentiated: Charging from the grid and charging using excess PV electricity. The second is defined as charging at times when local PV production exceeds local demand. Average daily charge and discharge patterns for the entire EV fleet of Singapore are shown in Fig. 9, with optimization results for the base scenario in Fig. 9a and for a high LSC scenario in Fig. 9b. In the base scenario, the two charging modes are clearly separated. Grid charging takes place almost exclusively during the night when

electricity prices are low. Excess PV is available during the day but in much smaller quantities. Only 2.21% of charging takes place using excess PV-power. V2G discharging takes place almost exclusively in the hour from 10:00 to 11:00 when electricity prices hit their highest point. The vast majority of annual charging electricity is consumed through driving, a fraction is lost during the charging process. Only 7.2% are discharged back into the grid. In the high LSC scenario, charging still took place primarily during the night and from the grid, however the fraction of charging from excess PV is increased to 18.7%. Discharging was spread more evenly with peaks during the morning and afternoon.

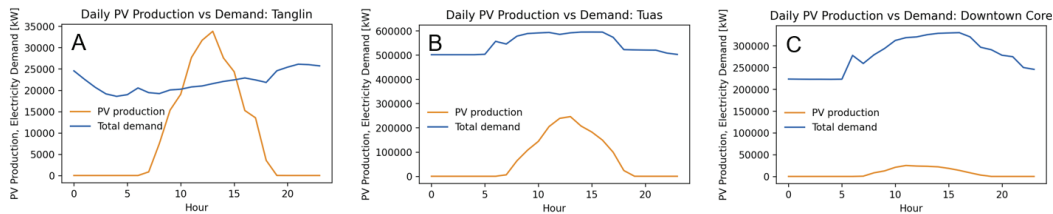


Figure 8: Average hourly building demand and PV production (capacities from base optimization) for three planning areas with three predominant sectors: Tanglin is residential (A), Tuas is industrial (B), Downtown Core is service dominated (C).

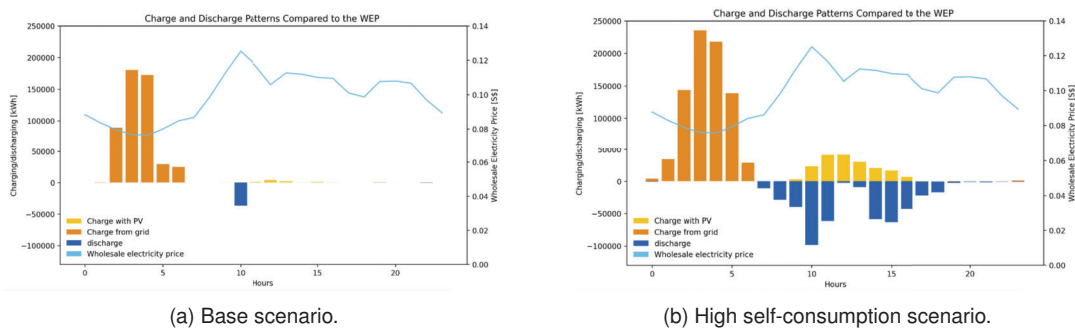


Figure 9: Average daily charging and discharging modes and patterns for EVs.

4. Discussion

Kobashi et al. (2020) [15] found that V2G in combination with PV systems could significantly reduce energy related costs and emissions in Kyoto. The difference in conclusions likely owes to both different model assumptions as well as real differences between the two locations. The most significant difference appears to be the result that local rooftop PV in Kyoto can cover approximately the entire annual electricity demand of the city. This means, times of overproduction are much more frequent and the possibility of storing electricity for later use becomes more valuable compared to this study, where PV generation rarely exceeded local demand. Kyoto is stated to have a rooftop area of 51.1 km² and an annual load of 8.1 TWh. In comparison, the area sum of the buildings in Singapore is 90.0 km² but the annual demand in 2019 was 51.7 TWh. This means that the demand per roof area is significantly higher in Singapore. Additionally, Kobashi et al. assume that 70% of roof area can be covered by PV whereas scaling factors used in this paper are significantly lower. Additionally, the study aggregates the city to a single unit. No transmission fees within the city are applied.

Schläpfer et al. (2021) [24] used the same mobility dataset and a similar method for extracting mobility patterns for Singapore. They also aggregated to the planning area level and found that for specific planning areas, up to 40% of nighttime household electricity demands could be covered by V2G, but for most districts this value was between 10% and 20%. These results were found using a first method assessment relying on a simple charging/discharging scheme where economic effects were excluded. Our study now investigated charging/discharging and PV capacity sizing based on a cost minimization. We found that under base assumptions for 2030 V2G under best case assumptions vehicle discharge made up 4% of the islands total demand (or 26% of household demand). However, cost optimal charging took place predominantly from the grid during night hours and discharging happened during the day. As such the transfer from PV electricity produced during the day to the night hours was not observed. Our results show that future work should also increase spatial resolution to better capture local mismatch of demand. This model assumes perfect foresight and focuses on overall economic optimization and not e.g. load balancing or individual benefits to stakeholders. Control schemes operating under bounded information and alternate optimization strategies could be explored.

5. Conclusion

This paper investigated the effects of electric storage from V2G technologies on optimal PV sizing on buildings and associated system costs and operational emissions at the district scale for the city of Singapore. Scenarios were based around the country's climate targets (Singapore Green Plan 2030). Energy and mobility flows were captured in an LP optimization model which defined PV scaling and charge/discharge patterns minimizing total systems cost. Carbon emissions were included in the form of a CO₂ tax. Three main inputs were generated: (i) City scale mobility patterns derived from a large set of mobile phone GPS records, (ii) energy demand at district level modeled using a bottom-up approach, and (iii) PV potentials using building geometries and 3D solar irradiation data. Different levels of local self-consumption were studied in a scenario analysis and compared to a base case.

Average self-consumption at the district level was very high in all scenarios; under base scenario assumptions it was 98% with a self sufficiency rate of 13%. These values were barely affected by V2G. In the best-case scenario with maximum PV installations average sufficiency increased to 18% and self-consumption at planning area scale dropped to 95% but with a significant range. In this scenario V2G was able to increase self-consumption by around 0.5%. Although impacts of V2G were low, the general expected effects were found. V2G was able to increase self-consumption and reduce exports to the grid. Reasons for low impact as compared to other studies are likely twofold. On the one hand Singapore's economically viable building PV potential is low compared to a relatively high demand. This means that PV only exceeds local demand in specific locations and times. Especially residential areas with a demand curve that is low and runs counter to PV production can generate significant overproduction and could be candidates for V2G. On the other hand, through the aggregation to the planning area level, local mismatches in production and demand were partially flattened and thus the potential for V2G to act as intermediate storage was reduced.

In order to gain further insight into the potential of V2G in cities like Singapore, future research could focus on improving mobility demand predictions, and combining large scale city dynamics with more fine-grained local analysis. Investigating additional cities could reveal location based effects. Finally, specific grid dynamics could be modelled explicitly to account for further benefits of V2G such as grid balancing and frequency regulation.

Acknowledgments

This research was conducted at the Future Cities Lab Global at Singapore-ETH Centre and ETH Zurich. Future Cities Lab Global is supported and funded by the National Research Foundation, Prime Minister's Office, Singapore under its Campus for Research Excellence and Technological Enterprise (CREATE) programme and ETH Zurich (ETHZ), with additional contributions from the National University of Singapore (NUS), Nanyang Technological University (NTU), Singapore and the Singapore University of Technology and Design (SUTD). Input was gratefully received from Luis Santos from the Cooling Singapore group at SEC on electricity modeling, and from Dr. Alina Galimshina from the Chair of Sustainable Construction at ETH on embodied emissions of PV systems. Acknowledgement also goes to Citydata for providing the mobility dataset and related support.

References

- [1] (SERIS) Solar Energy Research Institute of Singapore. *UPDATE of the Solar Photovoltaic (PV) Roadmap for Singapore*. Tech. rep. 2020. URL: [https://www.seris.nus.edu.sg/doc/publications/Update-of-the-Solar-Roadmap-for-Singapore-\(March-2020\).pdf](https://www.seris.nus.edu.sg/doc/publications/Update-of-the-Solar-Roadmap-for-Singapore-(March-2020).pdf).
- [2] Ayu Sukma Adelia. *Cooling Singapore project, retrieved from Openstreetmap, 2020*.
- [3] Energy Market Authority. *Energy Balance*. 2019. URL: <https://www.ema.gov.sg/singapore-energy-statistics/Ch04/index4> (visited on 03/08/2022).
- [4] Dominic Caviezel. "Sizing, Cost, and Emissions of Vehicle to Grid Coupled PV at District Scale". Master Thesis. ETH Zurich, 2022. URL: <http://hdl.handle.net/20.500.11850/595017>.
- [5] CITYDATA.ai. *Mobile Phone Records Singapore*. 2022. URL: <https://beta.citydata.ai/company/about> (visited on 03/08/2022).
- [6] Energy Market Company. *Price Information*. 2022. URL: <https://www.emcsg.com/marketdata/priceinformation> (visited on 03/08/2022).
- [7] Constance Crozier, Thomas Morstyn, and Malcolm McCulloch. "The opportunity for smart charging to mitigate the impact of electric vehicles on transmission and distribution systems". In: *Applied Energy* 268. December 2019 (2020), p. 114973. DOI: 10.1016/j.apenergy.2020.114973. URL: <https://doi.org/10.1016/j.apenergy.2020.114973>.
- [8] Igor Cvetkovic et al. "Future home uninterruptible renewable energy system with vehicle-to-grid technology". In: *2009 IEEE Energy Conversion Congress and Exposition, ECCE 2009*. IEEE, 2009, pp. 2675–2681. DOI: 10.1109/ECCE.2009.5316064.

- [9] Merkebe Getachew Demissie et al. "Inferring Passenger Travel Demand to Improve Urban Mobility in Developing Countries Using Cell Phone Data: A Case Study of Senegal". In: *IEEE Transactions on Intelligent Transportation Systems* 17.9 (2016), pp. 2466–2478. DOI: 10.1109/TITS.2016.2521830.
- [10] Reza Fachrizal and Joakim Munkhammar. "Improved photovoltaic self-consumption in residential buildings with distributed and centralized smart charging of electric vehicles". In: *Energies* 13.5 (2020). DOI: 10.3390/en13051153.
- [11] Jimeno A. Fonseca et al. "City Energy Analyst (CEA): Integrated framework for analysis and optimization of building energy systems in neighborhoods and city districts". In: *Energy and Buildings* 113 (2016), pp. 202–226. DOI: 10.1016/j.enbuild.2015.11.055.
- [12] Stephan Huber and Christoph Rust. "Calculate Travel Time and Distance with Openstreetmap Data Using the Open Source Routing Machine (OSRM)". In: *Stata Journal* 16.2 (2016), pp. 416–423. DOI: 10.1177/1536867X1601600209.
- [13] IEA. *Introduction to System Integration of Renewables*. CC BY 4.0. 2020. URL: <https://www.iea.org/reports/introduction-to-system-integration-of-renewables> (visited on 03/08/2020).
- [14] Md Shahadat Iqbal et al. "Development of origin-destination matrices using mobile phone call data". In: *Transportation Research Part C: Emerging Technologies* 40 (2014), pp. 63–74. DOI: 10.1016/j.trc.2014.01.002. URL: <http://dx.doi.org/10.1016/j.trc.2014.01.002>.
- [15] Takuro Kobashi et al. "On the potential of "Photovoltaics + Electric vehicles" for deep decarbonization of Kyoto's power systems: Techno-economic-social considerations". In: *Applied Energy* 275 (2020), p. 115419. DOI: <https://doi.org/10.1016/j.apenergy.2020.115419>.
- [16] Haiyang Lin et al. "The impact of electric vehicle penetration and charging patterns on the management of energy hub – A multi-agent system simulation". In: *Applied Energy* 230.May (2018), pp. 189–206. DOI: 10.1016/j.apenergy.2018.08.083. URL: <https://doi.org/10.1016/j.apenergy.2018.08.083>.
- [17] Rasmus Luthander et al. "Photovoltaic self-consumption in buildings: A review". In: *Applied Energy* 142 (2015), pp. 80–94. ISSN: 03062619. DOI: 10.1016/j.apenergy.2014.12.028. URL: <http://dx.doi.org/10.1016/j.apenergy.2014.12.028>.
- [18] Efstathios E. Michaelides. "Primary energy use and environmental effects of electric vehicles". In: *World Electric Vehicle Journal* 12.3 (2021). DOI: 10.3390/wevj12030138.
- [19] Portia Murray et al. "Optimal transformation strategies for buildings, neighbourhoods and districts to reach CO2 emission reduction targets". In: *Energy and Buildings* 207 (2020), p. 109569. DOI: 10.1016/j.enbuild.2019.109569. URL: <https://doi.org/10.1016/j.enbuild.2019.109569>.
- [20] Ministry of National Development et al. *SG Green Plan: Our Targets*. 2022. URL: <https://www.greenplan.gov.sg/targets> (visited on 03/08/2022).
- [21] Pedro Nunes, Raquel Figueiredo, and Miguel C. Brito. "The use of parking lots to solar-charge electric vehicles". In: *Renewable and Sustainable Energy Reviews* 66 (2016), pp. 679–693. DOI: 10.1016/j.rser.2016.08.015. URL: <http://dx.doi.org/10.1016/j.rser.2016.08.015>.
- [22] Gururaghav Raman and Jimmy Chih-Hsien Peng. "Electricity consumption of Singaporean households reveals proactive community response to COVID-19 progression". In: *Proceedings of the National Academy of Sciences of the United States of America*. Vol. 118. 34. 2021, pp. 1–7. DOI: 10.1073/pnas.2026596118.
- [23] Wolf Peter Schill and Clemens Gerbaulet. "Power system impacts of electric vehicles in Germany: Charging with coal or renewables?" In: *Applied Energy* 156.2015 (2015), pp. 185–196. DOI: 10.1016/j.apenergy.2015.07.012. URL: <http://dx.doi.org/10.1016/j.apenergy.2015.07.012>.
- [24] Markus Schläpfer et al. "Using Mobility Patterns for the Planning of Vehicle-to-Grid Infrastructures that Support Photovoltaics in Cities". In: (2021). arXiv: 2112.15006. URL: <http://arxiv.org/abs/2112.15006>.
- [25] Sriram Vaisambhayana and Anshuman Tripathi. "Study of electric vehicles penetration in Singapore and its potential impact on distribution grid". In: *2016 Asian Conference on Energy, Power and Transportation Electrification, ACEPT 2016*. IEEE, 2016, pp. 1–5. DOI: 10.1109/ACEPT.2016.7811513.
- [26] Mohammad M. Vazifeh et al. "Optimizing the deployment of electric vehicle charging stations using pervasive mobility data". In: *Transportation Research Part A: Policy and Practice* 121.January (2019), pp. 75–91. DOI: 10.1016/j.tra.2019.01.002. URL: <https://doi.org/10.1016/j.tra.2019.01.002>.
- [27] Christoph Waibel, Shanshan Hsieh, and Arno Schlüter. "Impact of demand response on BIPV and district multi-energy systems design in Singapore and Switzerland". In: *CISBAT 2021 International Conference Future Buildings and Districts*. Lausanne, Switzerland, 2021.